

## IMPROVING THE ACCURACY OF PIPING PROGRAMS WHEN ANALYZING CLOSELY COUPLED EQUIPMENT

**Michael A. Porter**  
Dynamic Analysis  
Leawood, Kansas

**Dennis Martens**  
The Pritchard Corporation  
Overland Park, Kansas

**Anthony C. Korba**  
The Pritchard Corporation  
Overland Park, Kansas

### ABSTRACT

Standard piping analysis programs, used to determine the deflections and stresses in piping systems, are often employed under conditions that are not within the scope of assumptions in the formulation of the programs. Such a case is the analysis of closely interconnected heat exchangers, pressure vessels and other such equipment. The major problem when using a piping analysis program is that the nozzle connections are modeled infinitely rigid rather than as an element with a finite flexibility. The results generated by such misapplication of the programs is usually (but not always) very conservative. This paper will demonstrate a hybrid method which employs conventional piping analysis software, WRC-107, WRC-297 and Finite Element (FE) software to attempt to obtain a better estimate of the deflections, forces, moments, and stresses. The results of the hybrid analysis are then compared to a complete FE analysis and a standard piping analysis of a sulfur recovery system. The indicated nozzle flexibilities and stresses varied considerably depending upon the analysis methodology used.

### DEFINING THE PROBLEM

The close coupling of piping and equipment for a Sulfur Recovery Unit (SRU) design raised concern that the normal methodology for studying piping flexibility would generate excessively conservative equipment nozzle loading data. The normal methodology used to model piping systems does not include nozzle stiffness information in the input data format. While this is adequate for normal piping configurations (where the piping provides the mechanism to absorb induced displacements), it was not considered adequate for closely coupled equipment. Normally equipment nozzles are modeled as either rigid or standard piping junctions which results in nozzle loads that do not adequately reflect the ability of the nozzle to rotate and displace. As pointed out in WRC-297 (Mershon et al., 1987), this was expected to produce inaccurate and conservative nozzle loadings.

An additional concern was that in the close coupled arrangement, an equipment nozzle that was inherently more rigid than another associated nozzle could result in a flawed analysis and possibly overload one of the nozzles.

To better define the loading on the equipment nozzles it became apparent that the nozzle stiffness would need to be included in the piping flexibility analysis. The piping flexibility software used was Caesar. This software accommodates modeling the nozzle stiffness when it is entered as spring rates at the nozzle-to-shell node.

Since the spring rates of the nozzles were unknown, it was decided to develop the nozzle-to-shell stiffness data using Algor, a Finite Element (FE) software package. The nozzle stiffness developed using the FE program would then be entered into the Caesar model.

To confirm the results of the Caesar flexibility analysis and the associated WRC-Bulletin 107 and WRC-Bulletin 297 nozzle stress information, the equipment and piping system would subsequently be modeled and analyzed using the FE software. This would provide a data comparison platform to review and verify the Caesar results and confirm the adequacy of this hybrid approach.

Subsequent to the development of the nozzle spring rates using the FE program, it was decided to determine the nozzle spring rates using WRC-Bulletin 297 and the ASME Section III, Division I, Paragraph NB-3686.5 procedures. These spring rates were then entered into the Caesar program to compute the associated forces and moments.

### PIPING FLEXIBILITY (CAESAR) MODEL

The initial piping model consisted of a 3 bed horizontal reactor, 2 vertical reheaters and 3 condensers. The reactor was restrained at the center in the axial direction and both saddles of the reactor were guided. The reactor was allowed to expand from the center outward toward the saddles. The condensers were located horizontally under the reactor. Two saddles supported the condensers. The saddle farthest from the reactor was modeled as an anchor and the saddle closest to the reactor was supported by a variable spring support. The reheaters were

located vertically above the outlet of the condensers and supported by variable spring supports. All of the equipment was connected by 20" diameter piping. (see Figure 1). Elements within the equipment were initially modeled as rigid joints.

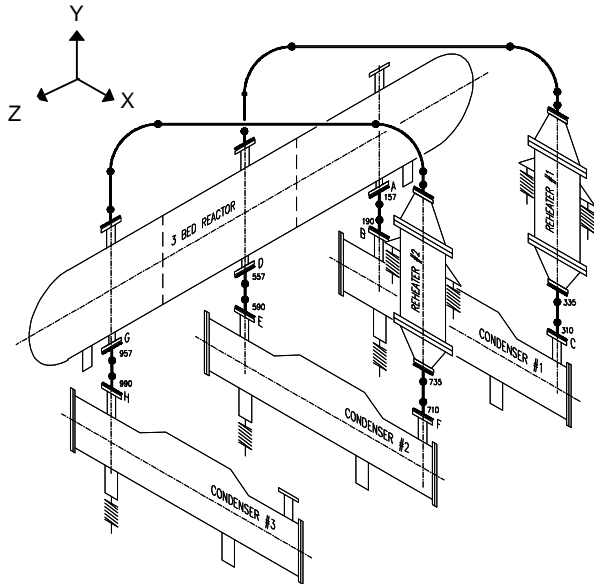


FIGURE 1 - SCHEMATIC OF PIPING MODEL

It became apparent after the first run that flexibility of piping as modeled would not accommodate the thermal displacements. The forces and moments at the connections between the pipe and the equipment nozzles were to be extremely high. Although indicated forces and moments were high at the pipe to equipment interfaces, the calculated stresses in the piping ranged between 3000 psi and 6000 psi, considerably lower than the allowable displacement stress of 29,000 psi allowed by ANSI B31.3.

In order to satisfy our concerns about the stresses developed at the equipment nozzle connections, a hybrid analysis method was developed. The method included modifying the original model by changing the equipment elements from rigid joints to pipe elements. In addition, a unique connecting node was placed at the nozzle and vessel interface. At each node, six restraints were added defining the flexibility of the nozzle (Caesar requires that all 6 fields be specifically identified as a spring rate or as rigid). The nozzle flexibility was calculated by means of a FE model using Algor software. The nozzle flexibility used was comprised of axial translations, circumferential and longitudinal bending. Shear and torsional stiffnesses were assumed rigid.

As a further means of comparing other methods to the FE analysis, the model above was changed to incorporate nozzle spring rates calculated by Welding Research Council Bulletin 297.

These nozzle spring rates were calculated using Caesar's built program, which calculates nozzle flexibilities based on the Welding Research Council Bulletin 297 procedure and automatically inserts the values into the model.

## FINITE ELEMENT (FE) MODEL

The FE model constructed for this analysis consisted of approximately 6750 isoparametric plate elements and 1440 beam elements. The plate elements were used to model the vessel and nozzle components. The beam elements were used for a variety of purposes: to model the pipe sections connecting the vessels, to model the tubes in the heat exchangers, to apply the load of the catalyst to the reactor vessel, and to serve as rigid connectors between the shell and reinforcement pads on the nozzles. The completed model, illustrated in Figure 2 with a section cut away so that the interior of the reactor may be seen, had approximately 41,500 degrees of freedom. The solution time on a 486-66 based PC was slightly over 2 hours.

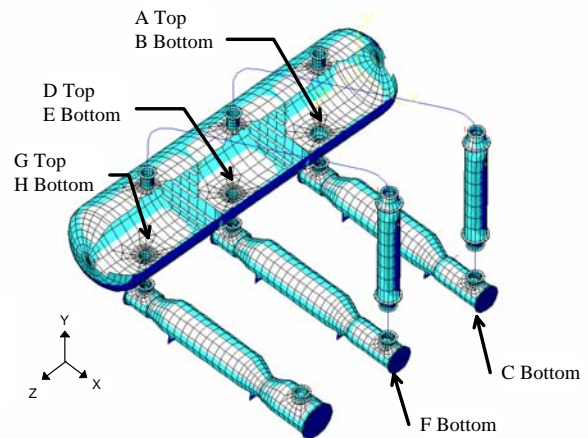


FIGURE 2 - FE MODEL WITH NOZZLES LABELED

In modeling the SRU system with the FE code, the modeling of the springs presented somewhat of a problem. Whereas most piping analysis codes are designed to arrive at an equilibrium position through an iterative procedure, most FE codes (including the code employed for this project) do not incorporate such a procedure. Thus it was necessary to apply balancing forces to the nodes where springs were modeled to provide the equilibrium balance. The process employed was to start with an initial force based upon the weight of each of the vessels and run the problem. The forces on the springs were then adjusted, based on the results of the analysis, and the solution process was repeated. Since the reactions of the various parts of the system were coupled, it took several iterations of this process to arrive at a balanced system.

## NOZZLE STIFFNESS COMPUTATION

Since a model of the entire system was constructed, the stiffness of the various nozzles were computed using the actual model geometry. If the complete system had not been modeled, the stiffness of each of the nozzles could have been computed using a relatively simple model constructed with parametric tools such as those produced by ATDAS (Advanced Technology Design & Analytical Services, Inc., Wethersfield, CT). Figure 3 illustrates such a model. The vessel portion of the model must be at least long enough to satisfy the attenuation length requirement

of the ASME code ( $2.5 * \sqrt{rt}$ ). The length of the nozzle is, for the most part, not important since the stiffness being computed is primarily that of the vessel shell.

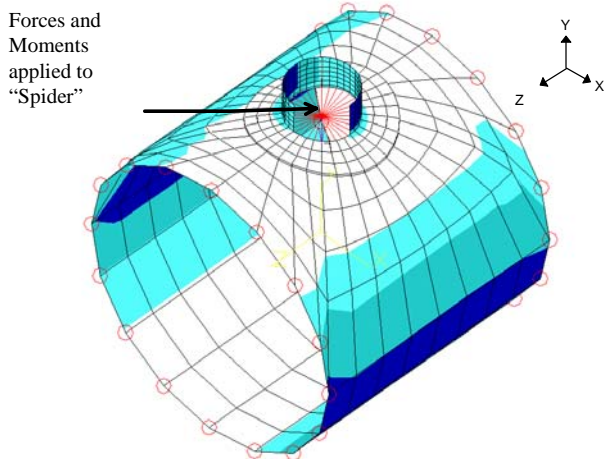


FIGURE 3 - "PARAMETRIC" MODEL OF NOZZLE

In the parametric models, the ends of the vessel portion of the models are fixed to prevent translations, while leaving the rotations free. This is similar to the approach that Mershon et al. (1987) detailed in the appendix of WRC-297. A "spider" of beam elements is constructed to connect all of the elements at the interior junction of the nozzle and vessel. Forces and moments may then be applied to this rigid "spider" to compute the resultant rotations and deflections. In order to avoid adding artificial stiffness to the vessel shell, it is important that the rigid "spider" elements not have a moment connection to the shell. In addition, the radial degree of freedom between the "spider" and the shell must not be constrained. With the FE code used, these requirements were met with the use of "End Releases" on the beam elements.

Since the nozzle and shell sizes are identical at both ends of the heat exchangers, the parametric models would indicate that the stiffnesses would be equal. The same would be true if the stiffnesses were computed using the formulas in ASME 1992 Section III, Division I - NB-3686.5 Branch Connections in Straight Pipe. When the complete FE model of the exchanger was used to compute the stiffnesses of the nozzles, they differed from the parametrically-derived values by approximately 50%.

The computed stiffnesses derived from the FE analysis, the WRC-297 procedure and a procedure proposed as an amplification of the WRC-297 procedure (Mokhtarian and Endicott, 1986) are tabulated in Table 1. The degree of agreement between the stiffness computation procedures used is less than encouraging.

Using the FE computed stiffnesses as a base, the stiffnesses computed with the ASME Section II NB-3686.5 procedure vary by a factor of somewhat less than 2 for the nozzles examined. These differences may be due to the apparent lack of provision for a reinforcing pad in the NB-3686.5 formulas. The stiffness computed with the WRC-297 procedure seem to be consistently low by a factor of approximately 2 in the circumferential direction. In the axial and longitudinal directions, such

consistency does not exist. It is interesting to note that the Mokhtarian procedure seems to work well only for nozzles A, D and G; for the other nozzles the comparison is not good at all.

The various parameters used by the various procedures are listed in Table 1. All of the nozzles examined appear to fall within the range of applicability stated in the respective procedures, although the limits are not clearly defined. WRC-297, for example, merely states that the procedure is good only for a limited range of geometries and does not define the geometries or the range.

### COMPARISON OF FE AND PIPING PROGRAM RESULTS

For the purpose of comparison with the piping model, the forces, moments, deflections and stresses at 10 locations in the FE and piping model are tabulated. These locations along with the node numbers associated with the piping model are indicated on Figure 1. The locations selected for reporting correspond to the face of the flange at the various nozzle connections, as illustrated on Figure 4.

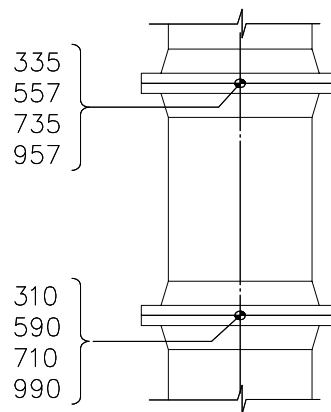


FIGURE 4 - TYPICAL PIPE/NOZZLE CONFIGURATION WITH NODE NUMBERING

Tables 2, 3 and 4 present the tabulated Displacement, Force and Moment data computed by both the piping analysis and by the FE analysis. Note that the column labeled "Orig. Pipe" represents the Caesar run with the nozzles considered rigid. The column labeled "Pipe+297" is the Caesar run with the nozzle stiffness computed with the WRC-297 procedure added. The column labeled "Pipe+FEA" is the Caesar run with the stiffnesses computed with the FE program added, while the column labeled "FE" is from the FE model alone.

The displacements computed by the several types of analyses are, for the most part, fairly close in value. In Table 2, however, we can see a fairly significant difference in the vertical (Y) deflection values on the reactor nozzle nodes. This difference is due to the way in which the reactor is treated by the two different programs types. The piping analysis program treats the reactor as a piece of pipe supported at the centroid. The FE program takes into account the fact that the vessel is supported only along the lower portion where it rests on the support.

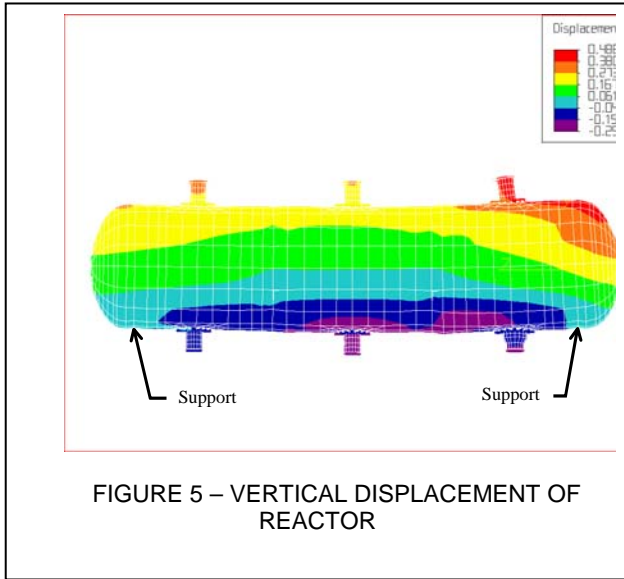


FIGURE 5 – VERTICAL DISPLACEMENT OF REACTOR

Figure 5 illustrates the deflected shape of the vessel with the magnitude of the deflection in the vertical direction indicated. Here we can see that there is localized deflection in the saddle support regions. This deflection is not seen by the piping analysis program. Additionally, in the FE analysis, the temperature variation (with elevation) in the reactor is modeled. Since the lower portion of the reactor is hotter than the upper portion, some of the “bowing” is due to the temperature gradient.

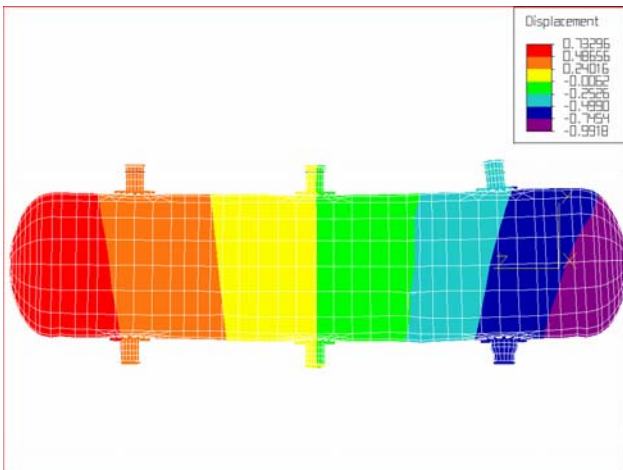


FIGURE 6 AXIAL DISPLACEMENT OF REACTOR

Figure 6 illustrates the deflected shape with the deflection in the axial direction indicated. The axial displacement is greater at the bottom of the vessel than at the top. This temperature effect is not accounted for in the piping program.

The way that the two programs handle the deflections of the various components leads to a more significant difference in the indicated forces and moments. As may be seen in Tables 3 and 4, the indicated forces and moments are not consistent between the two programs. In some cases, the forces reported by the

piping program tend to be conservative compared to those reported by the FE analysis; in other cases the opposite is true. There is a more significant variation in the moments reported by the two programs. From this limited analysis, it is unclear if there is a general correlation between the reported moments. While the overall highest moments are indicated by the piping program, there are individual location moments where the values reported by the piping program are considerably less than reported by the FE analysis.

The stresses in the nozzles were generally indicated to be quite low by the FE program. Table 5 shows the Stress Intensity indicated by the FE program at three selected nozzles on the reactor and the heat exchanger (see Figure 2 for the nozzle locations). Also indicated are the nozzle stresses which were computed using the forces and moments from the piping analysis as input to WRC-107 and WRC-297 (as would be customary for this type of vessel). For the most part, the stresses computed using either WRC-107 or WRC-297 tend to not be conservative when compared to the FE results unless the pad thickness is ignored. Ignoring the pad (as proscribed in the appendix of WRC-297) results in stresses which are quite conservative. Additionally, it should be noted that the stresses indicated here for WRC-297 are the shell stresses. If the WRC-297 nozzle stresses are examined, the degree of conservatism is even more pronounced. The apparent lack of agreement between the procedures seems to fall in line with the concerns recently raised by Dekker (1994) in his comparison of stress results from WRC-107 and Appendix G of BS 5500.

## RESULTS

The analysis indicated that the coupled equipment arrangement had adequate flexibility and that the equipment nozzle stresses were acceptable. The concern that the equipment nozzle (which was inherently more rigid than another associated equipment nozzle) could result in a flawed pipe stress analysis was determined to be unlikely.

The computed nozzle stiffness data developed by the different procedures and listed in Table 1, gives the authors concern in that the WRC-297 procedure yields nozzle-to-shell spring rates that range from 1/2 to over 10 times the FE-developed rates (the ratio is even higher in the axial direction). The ASME Division III procedures yield rates that range from 60% to 160% of the FE-developed rates. This disparity of spring rates would appear to be of such a magnitude that a piping analysis using the WRC or ASME data would yield a considerable variation in results.

The addition of the equipment nozzle stiffness information to the piping flexibility model resulted in a general reduction of the piping loads on the nozzles when compared to the original Caesar run, as is indicated in Tables 3 and 4. The data scatter is considerable and is similar to the type of scatter found in the computed spring rates.

The deviation of the developed Caesar modeled piping forces and moments using the WRC-297 spring rates compared to those developed using the FE spring rate data is considerable, but there is an apparent reduction in the major nozzle forces and moments. The comparison of these results to the results obtained from the FE analysis were in fair agreement, but considerable deviations

can be noted. The authors consider the FE model results to be the most accurate and can attribute some of the noted deviations to the FE model's ability to include equipment distortion in its analysis.

External Loadings", *Welding Research Council Bulletin No. 107*, August, 1965, revised March, 1979

#### AUTHORS' NOTES

Constructing models which yielded consistent results using the piping program and the FE program proved to be a difficult task. Numerous iterations of the programs were required to achieve the degree of agreement indicated in this paper. The differences in the coordinate systems used in WRC-107 and WRC-297 resulted in similar difficulties.

The authors recommend that when a vessel/piping system containing closely coupled vessels is analyzed, the engineer should incorporate nozzle flexibility in the analysis. The development of nozzle spring rates is best achieved with FE type of modeling. The use of WRC-297 or ASME Section III methods should be limited to applications where there is considerable margin between the calculated stresses and the allowable stresses.

The authors suggest that the engineer consider the use of parametric FE models to develop the nozzle stiffness data. These same models can be used to determine the nozzle shell and nozzle stress intensities using the forces and moments generated by the piping program. The nozzle stresses developed by the hybrid approach should be limited to approximately 1/2 the allowable design stress to compensate for the inaccuracies of the method. If it is necessary to determine the stresses more accurately, the authors suggest that the piping and associated vessels be modeled and analyzed using FE methods.

Finally, the authors would like to recommend that further investigation of the WRC-197 and WRC-297 stress results, as well as the WRC-297 and ASME Section II nozzle stiffness results, be considered. These widely used stress computation methods should be compared to available FE and laboratory data to insure the engineering community that adequate results are being obtained.

#### REFERENCES

- ASME Boiler and Pressure Vessel Code, Sec. III, Nuclear Power Plant Components, Div. 1, 1992, American Society of Mechanical Engineers, New York
- Dekker, C.L., 1994, "Comparison of local load stress calculation methods for nozzles on cylinders," *Int. J. Pres. Ves. & Piping*, Vol. 58, pp 203-213
- Mershon, J.L., Mokhtarian, K., Ranjan, G.V., and Rodabaugh, E.C., 1987, "Local Stresses in Cylindrical Shells Due to External Loadings on Nozzles - Supplement to WRC Bulletin No. 107 - (Revision I)," *Welding Research Council Bulletin 297*, September, 1987
- Mokhtarian, K., and Endicott, J.S., 1986, "Sensitivity Analysis of Flexibility at Cylinder-Cylinder Junctions," in *Design and Analysis of Plates and Shells*, G. E. O. Widera, H. Chung, D. Hui, eds, ASME Special Publication PVP-Vol. 105, American Society of Mechanical Engineers, New York, pp 65-69
- Wichman, K.R., Hopper, A.G., and Mershon, J.L., 1979, "Local Stresses in Spherical and Cylindrical Shells Due to

Table 1 - Computed Nozzle Stiffness

Nozzle	$\lambda$				Axial - lb/in			Ratios			
	d/D	r/t	L/(DT) <sup>2</sup>	d/(DT) <sup>1.5</sup>	FE	WRC-297	Mokhtarian	WRC/FE	Mok/FE		
A	0.188	37.16	8.27	1.63	9.39E+05	8.88E+06	2.20E+06	9.46	2.34		
B,E,H	0.488	13.67	5.13	2.63	4.34E+06	1.00E+10	1.48E+07	2306.00	3.41		
C,F	0.488	13.67	9.72	2.63	3.03E+06	1.00E+10	1.48E+07	3298.00	4.87		
D	0.139	42.67	11.61	1.29	1.73E+05	3.50E+06	1.60E+06	20.24	9.24		
G	0.139	42.67	8.85	1.29	3.48E+05	5.50E+06	1.60E+06	15.82	4.60		

Nozzle	$\lambda$				Circumferential - ft-lb/rad				Ratios			
	d/D	r/t	L/(DT) <sup>2</sup>	d/(DT) <sup>1.5</sup>	FE	WRC-297	Mokhtarian	ASME	WRC/FE	Mok/FE	ASME/FE	WRC/ASME
A	0.188	37.16	8.27	1.63	3.50E+07	1.78E+07	2.02E+07	2.60E+07	0.51	0.58	0.74	0.68
B,E,H	0.488	13.67	5.13	2.63	3.06E+07	1.24E+07	4.09E+07	3.11E+07	0.41	13.35	1.02	0.40
C,F	0.488	13.67	9.72	2.63	2.13E+07	1.24E+07	4.09E+07	3.11E+07	0.58	19.18	1.46	0.40
D	0.139	42.67	11.61	1.29	1.88E+07	1.00E+07	1.70E+07	1.12E+07	0.53	0.91	0.60	0.89
G	0.139	42.67	8.85	1.29	1.95E+07	1.00E+07	1.70E+07	1.12E+07	0.51	0.87	0.57	0.89

Nozzle	$\lambda$				Longitudinal - ft-lb/rad				Ratios			
	d/D	r/t	L/(DT) <sup>2</sup>	d/(DT) <sup>1.5</sup>	FE	WRC-297	Mokhtarian	ASME	WRC/FE	Mok/FE	ASME/FE	WRC/ASME
A	0.188	37.16	8.27	1.63	6.69E+07	1.78E+07	2.02E+07	2.60E+07	0.51	0.58	0.74	0.68
B,E,H	0.488	13.67	5.13	2.63	7.75E+07	1.24E+07	4.09E+07	3.11E+07	0.41	13.35	1.02	0.40
C,F	0.488	13.67	9.72	2.63	5.52E+07	1.24E+07	4.09E+07	3.11E+07	0.58	19.18	1.46	0.40
D	0.139	42.67	11.61	1.29	5.12E+07	1.00E+07	1.70E+07	1.12E+07	0.53	0.91	0.60	0.89
G	0.139	42.67	8.85	1.29	3.18E+07	1.00E+07	1.70E+07	1.12E+07	0.51	0.87	0.57	0.89

Table 2 - Computed Displacements

Node #	Deflection - X - IN				Deflection - Y - IN				Deflection - Z - IN			
	Orig Pipe	Pipe+297	Pipe+FE	FE	Orig Pipe	Pipe+297	Pipe+FE	FE	Orig Pipe	Pipe+297	Pipe+FE	FE
957	0.1139	0.1006	0.0888	0.0496	-0.0231	-0.023	-0.0208	-0.1177	0.4334	0.4327	0.4207	0.4519
990	0.1698	0.1351	0.1243	0.113	-0.1319	-0.1316	-0.1295	-0.2027	0.4168	0.4136	0.3234	0.4399
557	0.1127	0.0987	0.0888	0.0526	-0.0309	-0.0306	-0.0239	-0.2241	-0.0205	-0.0204	0.0196	-0.0011
590	0.1713	0.1323	0.1268	0.1419	-0.1607	-0.1604	-0.1537	-0.3236	-0.0301	-0.0306	-0.0269	0.0049
157	0.1245	0.1177	0.1033	0.0495	-0.0954	-0.0955	-0.0938	-0.1847	-0.6192	-0.6188	-0.621	-0.6072
190	0.187	0.1752	0.1574	0.1469	-0.2534	-0.2535	-0.2518	-0.3291	-0.6192	-0.6216	-0.5693	-0.6084
735	0.6594	0.5999	0.6171	0.734	0.3051	0.3064	0.3024	0.3537	0.0003	-0.0725	-0.0237	-0.0232
710	0.7325	0.6861	0.6862	0.8094	0.1885	0.1898	0.1859	0.2323	-0.0067	0.0635	-0.0272	-0.0095
335	0.709	0.6882	0.6815	0.7816	0.3705	0.3728	0.3713	0.386	-0.1629	-0.1665	-0.2272	-0.2077
310	0.7899	0.7753	0.7568	0.8488	0.2395	0.2418	0.2403	0.2508	-0.1304	-0.1344	-0.1768	-0.1674

Table 3 - Computed Forces

Node #	Force - X - LBS				Force - Y - LBS				Force - Z - LBS			
	Orig Pipe	Pipe+297	Pipe+FE	FE	Orig Pipe	Pipe+297	Pipe+FE	FE	Orig Pipe	Pipe+297	Pipe+FE	FE
957	2,602	-3,328	-3,920	-3,867	197	1,123	1,161	115	2,373	2,117	1,608	669
990	2,602	-3,325	-3,920	3,869	540	1,861	1,899	115	2,373	-2,117	-1,608	-669
557	4,183	-4,913	-4,643	-5,140	905	1,460	1,512	1,165	276	114	143	-157
590	4,183	-4,913	-4,643	5,140	1,643	2,198	2,250	1,165	276	114	143	157
157	1,597	-2,677	-2,027	-6,718	3,328	1,903	2,067	1,889	4,961	4,542	4,263	-3,771
190	1,597	-2,677	-2,027	6,718	4,022	2,597	2,761	1,889	4,961	4,542	4,263	3,771
735	253	-596	-310	1,395	254	347	277	356	114	92	178	-422
710	253	-596	-310	-1,395	609	-516	-587	356	114	92	178	422
335	907	199	270	2,097	203	369	207	349	220	361	329	-605
310	907	199	270	-2,097	660	-494	-656	349	220	361	329	605

Table 4 - Computed Moments

Node #	Moment - X - FT- LBS				Moment - Y - FT- LBS				Moment - Z - FT- LBS			
	Orig Pipe	Pipe+297	Pipe+FE	FE	Orig Pipe	Pipe+297	Pipe+FE	FE	Orig Pipe	Pipe+297	Pipe+FE	FE
957	20,428	18,266	13,012	-7,573	23,729	22,473	14,190	-50	22,278	-2,229	-6,609	-2,856
990	10,932	9,794	6,538	5,519	23,729	22,473	14,190	50	11,867	11,073	9,024	-9,025
557	4,859	-2,462	-1,374	-1,469	2,818	3,228	-120	-2,102	17,177	-988	-7,174	-2,684
590	3,754	-2,002	-800	1,953	2,818	3,228	-120	2,102	441	18,664	11,420	-13,100
157	45,768	-28,460	-23,843	27,858	65,663	-65,890	-53,016	56,100	19,130	5,444	10,834	-13,933
190	28,816	-12,940	-11,247	-15,600	65,663	-65,890	-53,016	-56,100	24,586	14,593	13,763	-7,910
735	3,594	-2,371	-1,884	367	2,114	3,883	2,793	3,499	6,049	1,364	-4,863	-7,828
710	2,967	-1,866	-903	1,941	2,114	3,883	2,793	-3,499	4,657	4,637	-3,157	15,458
335	10,338	-529	1,752	4,349	7,234	7,035	8,232	16,683	29,523	-14,262	-15,528	-12,000
310	11,550	1,457	3,558	-1,037	7,234	7,035	8,232	-16,683	34,505	-15,356	17,014	23,475

Table 5 - Nozzle Stress - psi, Computed using forces and moments from indicated analysis

Nozzle	FE Stress Intensity	Orig. Pipe			Pipe+297 Stiffness			Pipe + FE Stiffness			FE Only		
		WRC-107	WRC-297	WRC-297*	WRC-107	WRC-297	WRC-297*	WRC-107	WRC-297	WRC-297*	WRC-107	WRC-297	
A	13,345	5,573	6,302	33,077	3,762	4,488	33,077	3,435	4,089	19,447	4,159	5,231	23,288
B	9,013	7,801	17,074	83,079	3,726	4,773	30,065	3,867	5,231	28,736	6,272	7,104	59,589
C	6,351	4,948	7,910	40,298	2,361	3,487	18,245	2,638	3,883	20,490	3,746	5,947	29,069

WRC-297\* - Reinforcement thickness not included per Appendix A-5 Nozzle Reinforcement